

## Low-Temperature Nuclear Magnetic Resonance Studies of $\text{EuB}_6$

J. L. Gavilano,<sup>1</sup> B. Ambrosini,<sup>1</sup> P. Vonlanthen,<sup>1</sup> H. R. Ott,<sup>1</sup> D. P. Young,<sup>2</sup> and Z. Fisk<sup>2</sup>

<sup>1</sup>Laboratorium für Festkörperphysik, ETH-Hönggerberg, CH-8093 Zürich, Switzerland

<sup>2</sup>National Magnetic Field Laboratory, Florida State University, Tallahassee, Florida 32306

(Received 27 May 1998)

We report the results of  $^{153}\text{Eu}$  and  $^{11}\text{B}$  nuclear magnetic resonance (NMR) studies of  $\text{EuB}_6$  at temperatures above 0.04 K and in magnetic fields between 0 and 7 T. We have observed a surprising evolution of the  $^{153}\text{Eu}$  NMR spectrum at very low temperatures, which we interpret as evidence for a complex electronic ground state of  $\text{EuB}_6$ , involving the coexistence of two magnetically very similar, but electronically inequivalent, phases. The low temperature  $^{11}\text{B}$  NMR spectra reveal two inequivalent boron sites with internal fields of  $-0.02$  and  $-0.35$  T. [S0031-9007(98)07982-4]

PACS numbers: 75.30.Kz, 76.60.Cq

From the results of early work,  $\text{EuB}_6$  was thought to be a ferromagnetic semiconductor [1] with a Curie temperature of approximately 13 K involving the ordering of well-localized  $\text{Eu}^{2+}$  moments. However, this simple picture could not account for magnetic and electronic properties of this material [2–4]. For example, at low temperatures no insulating but rather a metallic behavior has been observed [5]. Also the magnetically ordered state of  $\text{EuB}_6$  has proven to be difficult to understand. Previous and more recent results [6,7] on the temperature dependence of the specific heat  $C_p(T)$  indicate that two consecutive phase transitions occur with onsets at 16 and 14 K, respectively. In an effort to add microscopic information to the database concerning the low-temperature behavior of  $\text{EuB}_6$ , we have made  $^{153}\text{Eu}$  and  $^{11}\text{B}$  NMR experiments on a  $\text{EuB}_6$  sample which has been characterized by structural, thermal, transport, and optical properties [6].

As the most surprising result we note an anomalous evolution of the  $^{153}\text{Eu}$  NMR spectrum at low temperatures, which implies the gradual development of a new ordered phase in  $\text{EuB}_6$  and the coexistence of two magnetically inequivalent phases in the ground state of this material. The differences appear to be minute and to consist of a rather subtle but distinct variation in the electronic environment at the Eu sites. Our  $^{11}\text{B}$  NMR results are consistent with a slight distortion of the crystal structure below the Curie temperature, but we have no evidence for moment reorientation phenomena at lower temperatures [7].

For our NMR experiments we used standard spin-echo techniques with external magnetic fields between 0 and 7 T, at temperatures between 0.04 and 300 K. The NMR spectra were measured at a fixed frequency by monitoring the spin-echo signal at a given frequency and varying stepwise the applied magnetic field. The spin-lattice relaxation time was measured by destroying the nuclear magnetization with a comb of rf pulses and observing the nuclear magnetization recovery towards thermal equilibrium. The spin-spin relaxation time  $T_2$  was obtained by analyzing the decay of the spin echo as a function of the separation between the rf pulses, using a model suggested for the case

of  $\text{EuO}$  by Barak and co-workers [8]. Prior to the actual NMR measurements we applied magnetic fields of the order of a few tesla at low temperatures, which, in the presence of even weak magnetic anisotropy, results in a very good alignment of the crystallites. Demagnetization fields produce magnetic inductions of the order of 1 T, comparable to the observed full widths of the various NMR lines.

In Fig. 1 we display examples of recorded  $^{153}\text{Eu}$  NMR spectra of  $\text{EuB}_6$  at temperatures between 0.08 and 2.15 K and at a fixed frequency of 156.36 MHz. Above 2 K the NMR spectrum consists of a single broad line (A in Fig. 1), but below 2 K an additional line (B in Fig. 1) appears. With decreasing temperature B gains in relative intensity, reaching a saturation value of approximately half of the total below 1 K. Considering the simple crystal structure of  $\text{EuB}_6$  a two-line  $^{153}\text{Eu}$  NMR spectrum is unexpected

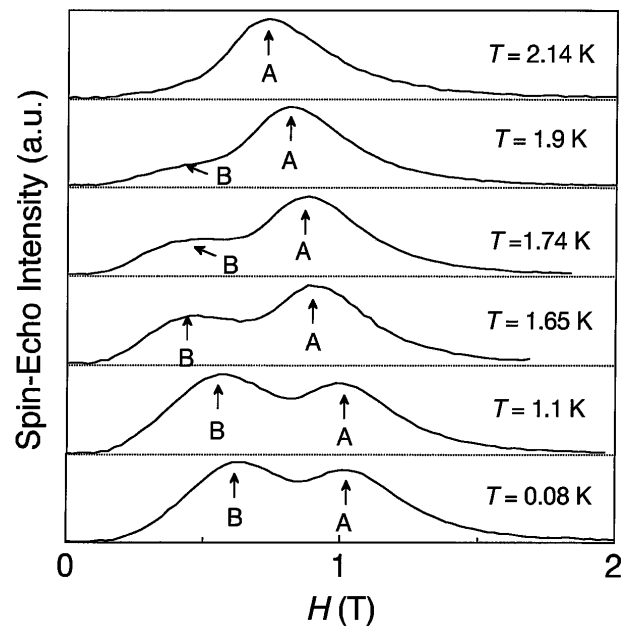


FIG. 1.  $^{153}\text{Eu}$  NMR spectra for  $\text{EuB}_6$  measured at various temperatures and a fixed frequency of 156.36 MHz. The data below 2 K show two broad peaks (A and B).

[9], and we are faced with the question of whether the two lines arise from inequivalent Eu sites within a single phase or from two different phases.

We consider the first possibility as rather unlikely because any temperature-induced lowering of the symmetry by lattice distortions generally yields a single Eu site and hence a single NMR line. The same applies for a simple reorientation of the ordered moments. A related scenario, considering different hyperfine fields of low-lying crystal-field split  $f$ -electron states is not compatible with our observation of two almost equally intense lines  $A$  and  $B$  even at the lowest temperatures.

The spectra thus give evidence for the existence of two phases in  $\text{EuB}_6$  below 2 K. We will refer to these phases simply as  $A$  and  $B$  corresponding to the lines indicated by  $A$  and  $B$  in Fig. 1. An analysis of the temperature dependence of the positions  $H(T)$  for both lines at three different frequencies (153.36, 156.36, and 157 MHz), using a spin-wave approximation of a Hamiltonian which contains only first and second Eu-Eu nearest neighbor dipolar and exchange interactions, yields the dispersion relation for magnon excitations  $\epsilon = \Delta + \epsilon_0 a^2 k^2$ , where  $\epsilon_0/k_B \cong 1.05$  K,  $a$  is the lattice constant, and  $\Delta/k_B$  is of the order of 1 K for both lines [10]. This suggests that the magnetic properties of both phases  $A$  and  $B$  are similar, and the small gap is consistent with a tiny distortion of the crystal structure.

At the lowest temperatures the hyperfine fields  $H_{\text{hf}}$  at the Eu nuclei are  $-34.54$  and  $-34.18$  T for the lines  $A$  and  $B$ , respectively. These negative hyperfine fields are similar to those of other ferromagnets involving the ordering of  $\text{Eu}^{2+}$  moments, such as  $\text{EuO}$  ( $-30.3$  T [8]) and  $\text{EuS}$  ( $-33.44$  T [11]). The negative sign of  $H_{\text{hf}}$  is consistent with a dominant contribution of the core polarization to the hyperfine mechanism, as expected for half-filled electron shells. The difference between the hyperfine fields of the lines  $A$  and  $B$  is too small to be associated with distinct changes of the valence of the Eu ions, but would indicate a difference in magnitude of the ordered moments in the two phases of the order of 1%.

Unusual features are also observed in the transversal relaxation time  $T_2$  of  $^{153}\text{Eu}$  in  $\text{EuB}_6$ , and below we discuss in some detail why they support our interpretation of two coexisting magnetic phases. In Fig. 2 we present examples of nuclear spin-echo-decay curves for  $^{153}\text{Eu}$  in  $\text{EuB}_6$  measured at 156.36 MHz and  $T = 1.47$  K for three different fields. The echos have been normalized to have the same intensity at the shortest delay. The curves do not have a single-exponential functional form but give evidence for a distribution of  $T_2$ 's. Although, from these data, it is clear that the transverse relaxation is not constant across the spectrum (compare curves I, II, and III), a quantitative analysis is complicated because it relies on data from the tail ends of the echo-decay curves that are accessible in our experiments.

Non-single-exponential echo-decay curves are common in ferromagnets [8] and have been attributed to micro-

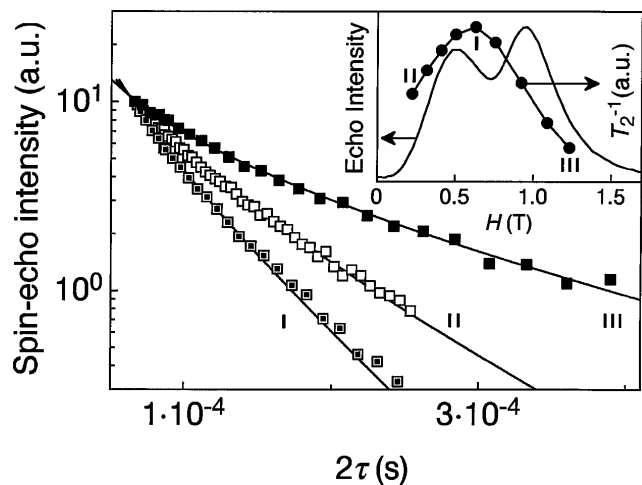


FIG. 2. Echo-decay curves of  $^{153}\text{Eu}$  in  $\text{EuB}_6$  at 1.47 K measured at applied magnetic fields of 0.22 (I), 0.63 (II), and 1.23 T (III). The solid lines represent fits to the data described in the text. The inset shows the  $^{153}\text{Eu}$  NMR spectrum for  $T = 1.47$  K with the corresponding  $T_2^{-1}$  profile. The singular values of  $T_2^{-1}$ 's related with the echo-decay curves of the figure are also indicated. Note that the minimum of the spectrum does not coincide with the maximum of  $T_2^{-1}$  (see text).

scopic inhomogeneities, which produce a microscopic distribution,  $g(\nu - \nu_0)$ , of Larmor frequencies  $\nu$ . The center  $\nu_0$  of the distribution is a random variable characterizing different local environments but its width is taken to be the same over the whole sample. The width of  $g(\nu - \nu_0)$  is closely related to the distribution of hyperfine fields caused by strains, impurities, and other microscopic imperfections [8]. The changes of the Zeeman energy levels of neighboring spins reduce the possibilities of mutual spin flips and, thus, for a given nucleus,  $1/T_2$  is reduced to a fraction proportional to (i) the number of nearby nuclear spins with a similar Zeeman energy, given by  $g(\nu - \nu_0)$ , and (ii) the strength of the spin-spin interaction  $B_{i,j}$  which can compensate energy differences. In ferromagnets  $B_{i,j}$  can be rather large because it has a contribution which involves the exchange of virtual magnons [12,13]. Since, in addition, microscopic inhomogeneities can lead to large changes in the local fields at neighboring sites, one expects for ferromagnets a distribution of the transverse relaxation of the form  $(1/T_2^{(0)})g(\nu - \nu_0)$ , with  $g$  normalized so that  $1/T_2^{(0)}$  is the maximum rate. In the limit of a very broad NMR line  $G(\nu)$ , whose shape is determined by macroscopic inhomogeneities, the spin-echo intensity  $A(t, \nu)$  has a time decay of the form [8]

$$A(t, \nu) \propto \int_{-\infty}^{\infty} d\nu_0 g(\nu - \nu_0) \times \exp[-t(1/T_2^{(0)})g(\nu - \nu_0)]. \quad (1)$$

Following Barak and co-workers [8] we have chosen a Lorentzian distribution  $g(\nu - \nu_0)$  of Larmor frequencies. Equation (1) is used to fit the echo-decay data with two

free parameters,  $1/T_2^{(0)}$  and an overall scaling factor absorbing the width of  $g(\nu - \nu_0)$ . Examples of best fits are displayed in Fig. 2 by the solid lines. To simplify the notation we will refer to  $1/T_2^{(0)}$  as  $T_2^{-1}$ .

Although, the above analysis is based on the tails of the echo-decay curves accessible in our experiments, we trust our approach to be reliable. The employed model is based on reasonable assumptions and has successfully been used in the past to analyze data on related ferromagnets [8]. The derived values of  $T_2^{-1}$  reflect very well the qualitative behavior of the echo-decay curves; they are always found to be larger for faster relaxations (see Fig. 2). After correction for the inhomogeneous echo decay using Eq. (1), the integrated NMR intensity  $\mathcal{A}$  multiplied by the temperature  $T$  is, as expected, roughly  $T$  independent. In particular, for temperatures between 1 and 2 K, where drastic changes of the  $^{153}\text{Eu}$  NMR spectrum occur,  $\mathcal{A}T$  changes less than 10%. This seems to rule out possible systematic errors and adds confidence to our approach.

In Fig. 3 we show  $T_2^{-1}$  as a function of the applied field for a fixed frequency of 156.36 MHz and several temperatures.  $T_2^{-1}$  increases with decreasing fields and has, if any, only a weak  $T$  dependence in the region where the signal corresponding to phase A dominates. However, at lower fields, in the region where the B phase intensity is dominant,  $T_2^{-1}$  decreases with decreasing applied fields and exhibits a strong  $T$  dependence. These anomalous field and temperature behaviors are again consistent with the gradual formation of a new phase B at low temperatures, whereas the manifestation of phase A (NMR spectrum,  $T_2$ ) seems to continue as established at higher temperatures. In the inset of Fig. 3 we display the  $T_2^{-1}(H)$  profile for 0.08 K. Here and in the inset of Fig. 2 one observes that the maxi-

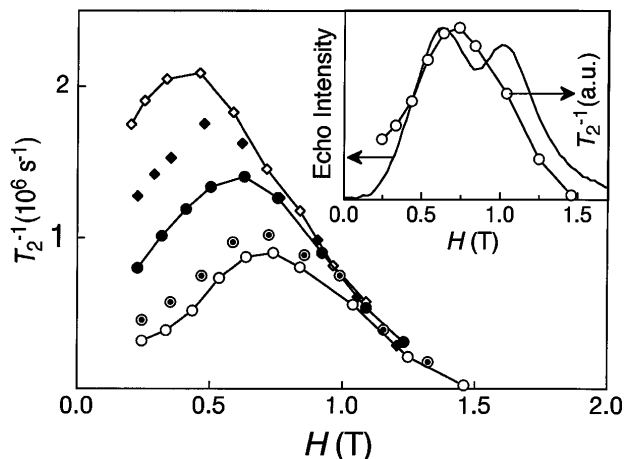


FIG. 3.  $T_2^{-1}$  as a function of the applied field for  $^{153}\text{Eu}$  in  $\text{EuB}_6$  measured at 156.36 MHz and temperatures (from top to bottom) of 1.82, 1.65, 1.47, 1.1, and 0.08 K. The solid lines are to guide the eye. The inset shows the  $^{153}\text{Eu}$  NMR spectrum and the corresponding  $T_2^{-1}$  profile for  $T = 0.08$  K. Note that the minimum of the spectrum does not coincide with the maximum of  $T_2^{-1}$ .

mum of  $T_2^{-1}$  does not coincide with the intensity minimum near the center of the NMR spectrum, but is shifted towards the maximum of line B. The same is true for all the temperatures, where line B can be identified, and therefore it is rather unlikely that line B is a simple  $T_2$  artifact, in the sense that a large value of  $T_2^{-1}$  at a particular point of the resonance could lead to an apparent reduction in signal intensity because the fast relaxation would wipe out the signal before its acquisition begins. As may be seen in Fig. 3, the changes of  $T_2^{-1}$  across the spectrum are much more distinct for higher than for lower temperatures. Hence, artificial  $T_2$  induced effects would be expected to be more pronounced at higher temperatures, contrary to what we observe. The necessary corrections of the NMR spectra for the nonzero and inhomogeneous  $T_2^{-1}$  leave the corrected  $^{153}\text{Eu}$  NMR spectra with the two-peak feature.

In Fig. 4 we display the corrected relative NMR intensity of line B as a function of temperature at a frequency of 156.36 MHz (circles). Changing the resonance frequency does not significantly affect the relative intensity of phase B, and the NMR spectrum collected at a fixed magnetic field, varying stepwise the frequency, has the two-line pattern similar to those plotted in Fig. 1 [10].

Additional experiments monitoring the NMR of  $^{11}\text{B}$  have been made, and their results will be published in detail elsewhere [10]. Here we note only that the  $^{11}\text{B}$  spectra reveal two maxima implying two slightly different hyperfine fields at the boron sites but show no significant variation with decreasing temperature below 3 K. The observed splitting of the  $^{11}\text{B}$  NMR spectra is most easily reproduced by assuming that the Eu moments are oriented along the  $\langle 110 \rangle$  direction, resulting in direct dipolar fields  $H_d = -0.117$  T at four of the boron sites and  $H_d = 0.234$  T at the remaining two, respectively. To reproduce the observed resonant fields an additional hyperfine transferred field of  $-0.23$  T for all boron sites has to

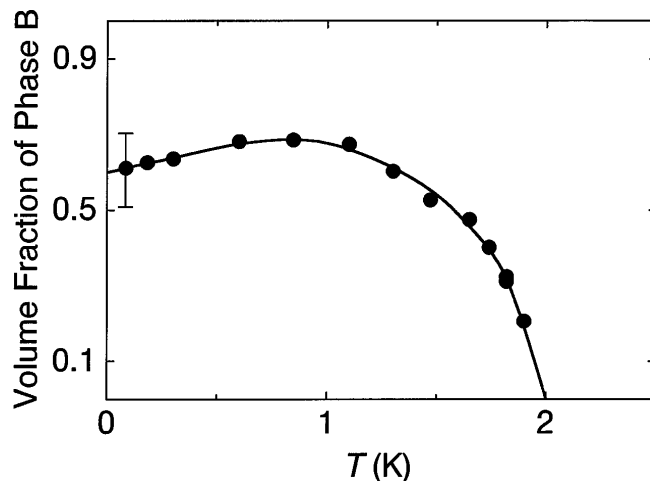


FIG. 4. Temperature dependence of the relative NMR intensity of peak B corrected for  $T_2$  effects. The filled circles represent data measured at 156.36 MHz. The solid line is a guide to the eye.

be assumed. For this or any other moment orientation, we cannot exclude, however, that a slight distortion of the crystal lattice is responsible for the shape of the  $B$  spectra. Since the temperature dependence of the  $^{11}\text{B}$  NMR spectra does not change significantly below 3 K we may exclude moment reorientations or considerable alterations of electronic densities to be the cause for the appearance of the two inequivalent phases presented above. The insensitivity of the boron spectra to the onset of a second magnetic phase below 2 K is attributed to the much weaker hyperfine coupling of the  $B$  nuclei to the Eu  $f$ -electron moments in comparison with the corresponding coupling of the Eu nuclei and the only tiny difference in the moment size between phases  $A$  and  $B$  mentioned above.

A similar conclusion may be reached from our results for the spin-lattice relaxation rate measured at the boron sites. They reveal no significant anomalies in  $T_1^{-1}(T)$  below 5 K [10], again indicating that the previously discussed low-temperature features of  $\text{EuB}_6$  do not substantially change the microscopic electronic environments of the boron sites.

Since the results for the  $^{11}\text{B}$  NMR give no hint for significant changes at low temperatures, we have to conclude that phase  $B$ , detected in the results of  $^{153}\text{Eu}$  NMR, is not very different from phase  $A$ , which is present already at higher temperatures. This in turn leads to the question of what causes two coexisting similar phases in  $\text{EuB}_6$ ? It is natural to attribute the differences of these phases to weak terms in the electronic Hamiltonian, which either violate an important symmetry or act only through a higher-order perturbation process. Spin-orbit and crystal-field interactions, acting weakly on the  $\text{Eu}^{2+}$  ions, are the prime candidates for such a mechanism. Their main role would not just be to lift the degeneracy of the  $4f^7$  ground state, but to induce two slightly different ground states. In any case our findings point to a delicately balanced situation for the ground state of  $\text{EuB}_6$ .

In conclusion, the results for the  $^{153}\text{Eu}$  NMR spectra at very low temperatures, well within the ferromagnetic state of  $\text{EuB}_6$ , signal the gradual development of a second ordered phase. The  $^{11}\text{B}$  NMR results seem to rule out spin reorientation phenomena in  $\text{EuB}_6$ , at least for applied fields of the order of 1 T or more, but they would allow for a small lattice distortion below the Curie temperature. Possible lattice distortions are of interest here in connection with electron-lattice interactions influencing the properties of  $\text{EuB}_6$ , particularly in view of the transition to a ferro-

magnetic state and the concomitant dramatic reduction of the electrical resistivity [5], similar to what is observed at higher temperatures in manganese oxides [14]. Phase separation phenomena have recently become of interest in connection with transition metal oxides [15,16] and high- $T_c$  superconductors [17]. It remains to be seen whether our observation reflects similar physics in this hexaboride compound.

This work was financially supported by the Schweizerische Nationalfonds zur Förderung der Wissenschaftlichen Forschung.

- 
- [1] B. T. Matthias, Phys. Lett. **27A**, 511 (1968).
  - [2] J. Etourneau and P. Hagenmuller, Philos. Mag. **52**, 589 (1985).
  - [3] M. Kasaya, J. M. Tarascon, J. Etourneau, and P. Hagenmuller, Mater. Res. Bull. **130**, 751 (1978).
  - [4] Z. Fisk, D. C. Johnston, B. Cornut, S. von Molnar, S. Oseroff, and R. Calvo, J. Appl. Phys. **50**, 911 (1979).
  - [5] C. N. Guy, S. von Molnar, J. Etourneau, and Z. Fisk, Solid State Commun. **33**, 1055 (1980).
  - [6] L. Degiorgi, E. Felder, H. R. Ott, J. L. Sarrao, and Z. Fisk, Phys. Rev. Lett. **79**, 5134 (1997).
  - [7] S. Süllo, I. Prasad, M. C. Aronson, J. L. Sarrao, Z. Fisk, D. Hristova, A. H. Lacerda, M. F. Hundley, A. Vigliante, and D. Gibbs, Phys. Rev. B **57**, 5860 (1998).
  - [8] J. Barak, I. Siegelstein, A. Gabai, and N. Kaplan, Phys. Rev. B **8**, 5282 (1973).
  - [9] In addition to  $^{153}\text{Eu}$ , there is the  $^{151}\text{Eu}$  isotope in similar natural abundance. However, its signal lies far away. Also far away in field are the corresponding  $^{11}\text{B}$  and  $^{13}\text{B}$  NMR signals.
  - [10] B. Ambrosini, J. L. Gavilano, P. Vonlanthen, and H. R. Ott (unpublished).
  - [11] M. W. Pieper, J. Kötzler, and K. Nehrke, Phys. Rev. B **47**, 11 962 (1993).
  - [12] T. Nakamura, Prog. Theor. Phys. **20**, 547 (1958).
  - [13] H. Suhl, J. Phys. Radium **20**, 333 (1959).
  - [14] See, e.g., Y. Tokura, Curr. Opin. Solid State Mater. Sci. **3**, 157 (1998), and references therein.
  - [15] V. J. Emery, S. A. Kivelson, and O. Zachar, Phys. Rev. B **56**, 6120 (1997).
  - [16] J. M. Tranquada, P. Wochner, and D. J. Buttrey, Phys. Rev. Lett. **79**, 2133 (1997).
  - [17] See, e.g., *Phase Separation in the Cuprate Superconductors*, edited by K. A. Müller and G. Benedek (World Scientific, Singapore, 1993).